ISSN 1063-7737, Astronomy Letters, 2008, Vol. 34, No. 2, pp. 133–140. © Pleiades Publishing, Inc., 2008.
Original Russian Text © N.I. Kobanov, D.Yu. Kolobov, S.A. Chupin, 2008, published in Pis'ma v Astronomicheskiĭ Zhurnal, 2008, Vol. 34, No. 2, pp. 152–160.

Traveling Waves in the Sunspot Chromosphere: Problems and Puzzles of Experiments

N. I. Kobanov*, D. Yu. Kolobov, and S. A. Chupin

Institute of Solar–Terrestrial Physics, Russian Academy of Sciences, Siberian Branch, P.O. Box 4026, Irkutsk, 664033 Russia

Received August 14, 2007

Abstract—The difficulties of the primary interpretation of wave processes observed in the sunspot chromosphere are discussed. Frequency filtering is shown to be helpful in revealing traveling waves more clearly, which eventually affects the objectivity of estimating their parameters. The measured horizontal phase velocities are 40–70 km s^{-1} for umbrae and 30–70 km s^{-1} for penumbrae. Analysis of high-cadence observations has revealed an altitude inversion of the spatial localization of the three-minute oscillation power. It is pointed out that the pattern of umbral traveling waves is not constant and periodically gives way to the pattern of standing waves.

PACS numbers : 96.60.-j; 96.60.Na; 96.60.qd
DOI: 10.1134/S1063773708020060

Key words: *solar chromosphere, umbral oscillations, running penumbral waves.*

INTRODUCTION

The oscillations and traveling waves in the sunspot chromosphere have been actively studied since their discovery (Beckers and Tallant 1969; Giovanelli 1972; Zirin and Stein 1972). The three-minute oscillations in the umbral chromosphere were first detected as periodic brightenings (Beckers and Tallant 1969), hence their name "umbral flashes." The fact that the three-minute oscillations and umbral flashes are a manifestation of the same process was not immediately understood. Some authors consider them to be standing acoustic waves (Christopoulou et al. 2000; Georgakilas et al. 2000), while others believe that these oscillations propagate into penumbrae, giving rise to running penumbral waves (Zirin and Stein 1972; Tziotziou et al. 2002).

A new stage in these studies began when satellite information about the oscillations in the upper chromosphere, the transition zone, and the solar corona became available (Banerjee et al. 2002; O'Shea et al. 2002; Brynildsen et al. 2003, 2004; Doyle et al. 2003). Nevertheless, the connection between the three-minute umbral oscillations and running penumbral waves (RPWs) remains the most acute problem to date. Two ideas attempting to explain the observed facts have gained acceptance. According to one of them, the running penumbral waves are a direct extension of the umbral three-minute traveling waves (Tziotziou et al. 2002). According to the second idea, there is no actual wave propagation in the horizontal direction at all, but there is an apparent pattern due to the fact that the oscillations propagating along different magnetic field lines experience a time delay proportional to the path length (Rouppe van der Voort 2003). In this case, it is assumed that the oscillations at the bases of all magnetic flux tubes are excited almost simultaneously and that their propagation velocity is the same in all flux tubes. The "piston-like" motions of a convective cell can act as a general excitation source. Given the universally accepted topology of the magnetic field in a single regular (circular) sunspot, the farther the observed point from the geometric center of the sunspot, the larger the phase delay of the line-of-sight velocity signal.

In the literature, the former and latter ideas are commonly called, respectively, a "trans-sunspot wave" and a "visual pattern" (see, e.g., Tziotziou et al. 2002).

Currently available observations continue to reveal a fairly complex situation with the propagation of waves in the sunspot chromosphere. Many authors commonly assume that the frequency of traveling waves decreases as they propagate from the umbra into to the outer penumbra. A similar effect is also found in the measurements of the propagation velocity of traveling waves. According to these views, the latter decreases from 20 km s^{-1} at the umbral

*E-mail: kobanov@iszf.irk.ru

boundary to 10–15 km s^{-1} at the outer penumbral boundary (Tziotziou et al. 2006, 2007).

On the other hand, using currently available methods, a number of authors have shown that the running penumbral waves are *not* an extension of the three-minute umbral waves. The measured propagation velocity of the umbral waves turned out to be much higher, 40–70 km s^{-1} (Kobanov and Makarchik 2004; Kobanov et al. 2006).

Thus, we see that there is a considerable spread in the measurements of the horizontal oscillation propagation velocity (irrespective of whether these waves are real or apparent). This necessitates invoking observational data that would make the inadequacy of the primary interpretation of observations less likely.

To solve the question of what we are dealing with in reality, we must have reliable information about the main parameters of the traveling waves in the sunspot chromosphere. These include the line-of-sight velocity amplitude, frequency, horizontal phase velocity, and spatial localization of the traveling waves.

The goal of this paper is to compare our own latest results with those of other authors and to draw the attention of researchers to the most acute aspects of the problem of traveling waves in sunspots.

THE INSTRUMENT AND THE METHOD

The observational data analyzed here were obtained with the horizontal solar telescope of the Sayan Solar Observatory located at an altitude of 2000 m. At a primary mirror diameter of 900 mm, the telescope has a theoretical resolution of about 0.″2. Unfortunately, this telescope is not yet equipped with adaptive optics and the Earth's atmosphere degrades this parameter by a factor of 4–5. The photoelectric guide of the telescope is capable of tracking the solar image with an error of 1″ for several hours of observations. In our observations, we used a Princeton Instruments CCD array thermoelectrically cooled to −40°C. One CCD pixel corresponds to 0.″2. Rotating the CCR array by 90°, we could set either a 60″ or 250″ field of view. In the latter case, the observed segment of the spectrum was reduced by a factor of 4. For convenient positioning of the object at the spectrograph entrance slit, we used a Dove prism.

The WinSpec software package of the same company was used to control the CCD array during our observations. Usually, we cut out the region of interest from the CCD spectrum. This operation reduced significantly the size of the file being saved. We applied 2- and 4-pixel binning, limiting the spatial resolution to 0.″5–1″ depending on the observing conditions. As a result, we were able to write time series up to several hours in duration into a file. Using external synchronization, we could regulate the rate of exposure from 5 frames per second to 6 frames per minute, in accordance with the observational task and atmospheric conditions. At considerable atmospheric jitter, there was a risk that high frequencies would penetrate into low ones, the so-called stroboscopic effect. To suppress this effect, the "dead" time intervals between the exposures should be at a minimum (preferably no longer than a quarter of the exposure time). Occasionally, the exposure had to be artificially increased by inserting neutral filters.

The series of spectrograms obtained in a normal mode allowed us to measure the line-of-sight velocity and intensity. When polarization optics was installed, the longitudinal magnetic field strength was additionally measured (Kobanov 2001).

This paper is based on simultaneous observations in the Hα 6528 Å and FeI 6569 Å lines with a cadence of 0.5 s. The telluric line near Hα was used to eliminate the spectrograph noise. The Doppler velocity was determined as the difference between the intensities in the red and blue wings of the spectral line profile normalized to their sum. Most of the measurements were performed in H$\alpha \pm 0.2$ Å (chromosphere) and FeI 6569 Å $\pm$ 0.15 Å (photosphere). The processed data sets were then used to construct half-tone space–time diagrams, Fourier spectra, and wavelet diagrams. The applied frequency filtering was helpful in revealing the properties of individual oscillation modes, which were chosen by analyzing the Fourier spectrum. For this purpose, the original data sets were subjected to a direct wavelet transform, in which the frequency of interest was selected, and the original distribution for the selected frequency was reconstructed using the inverse wavelet transform. The derived distribution was then used to construct filtered Doppler velocity diagrams.

RESULTS AND DISCUSSION

Umbral Waves

The chevron structures in the space–time half-tone line-of-sight velocity diagrams are simple and reliable tracers of umbral traveling waves (Kobanov et al. 2006). The oscillation propagation velocity can be easily determined from the slope of the chevron wings with almost the same accuracy as it can from the phase delay of the Doppler velocity signal measured in different parts of the umbra (Fig. 1).

It is appropriate to compare our results with the most recent data by Tziotziou et al. (2006, 2007). First of all, it should be noted that the horizontal phase velocity of the three-minute oscillations we measured, 40–70 km s^1, is considerably higher than

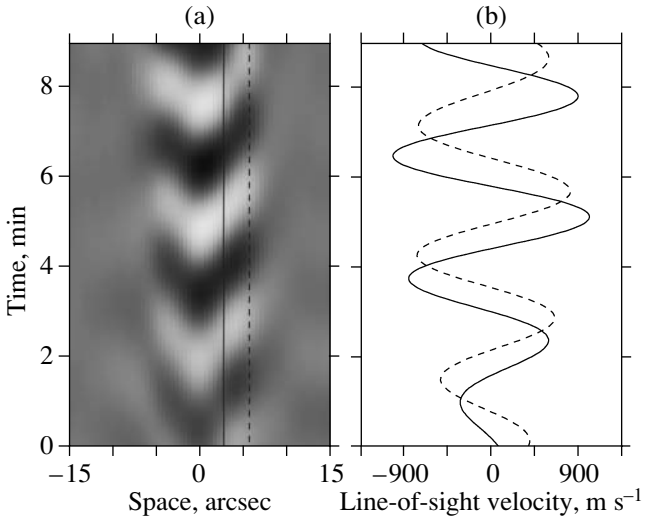

Fig. 1. Three-minute line-of-sight velocity mode in the chromosphere of the sunspot NOAA 791. (a) Chevron structures representing traveling umbral waves; the dark and light areas correspond to the velocities directed away from and toward the observer, respectively. (b) Phase delay between the Doppler velocity signals at the points of 6″ and 3″ marked by the vertical lines in Fig. 1a.

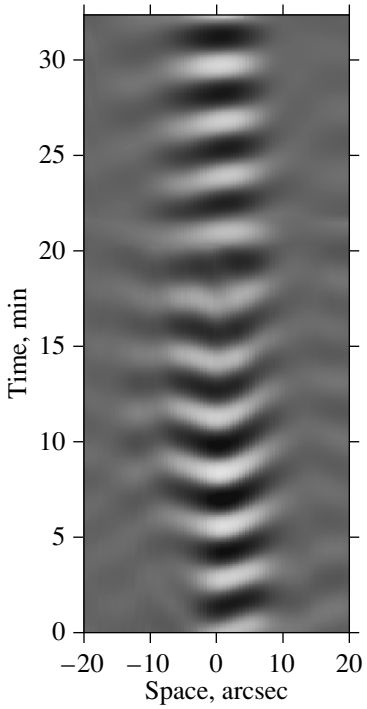

Fig. 2. Example of the alternation of traveling (chevron pattern) and standing (horizontal bands) umbral waves.

that found by these authors. According to the measurements by Tziotziou et al. (2006, 2007), the umbral wavefront velocity does not exceed 20 km s¹ near the umbral boundary.

Another peculiarity is that, according to our observations, the traveling waves traced by the chevron structures occupy a smaller part of the entire period during which the three-minute oscillations are observed. Distinct chevron structures often give way to almost horizontal bands in the half-tone line-of-sight velocity diagrams (Fig. 2). This position of the bands suggests a very high horizontal phase velocity, which may be indicative of the presence of standing waves at these times. Standing waves could appear if the transparency conditions for the chromosphere–transition zone boundary changed for some reasons and a considerable fraction of the waves were reflected back.

Let us assume that we observe acoustic waves propagating along the magnetic field lines. In this case, the line-of-sight velocity oscillations can be reliably recorded by the Doppler shift of a spectral line. The subsequent analysis was performed in terms of the "visual pattern" scenario. The phase delay of the line-of-sight velocity signal measured in the horizontal direction can arise, because the inclination of the magnetic field lines increases from the umbral center to the boundary. Let us attempt to roughly estimate the minimum depth required for the accumulation of the measured phase difference. The inclination of the magnetic field lines to the vertical line at the umbral boundary is known to be about 30°. Let us assume that this inclination is retained along the entire path where the main signal delay takes place, including the altitudes observed in Hα. This assumption minimizes the path length, since the inclination angle actually decreases with depth smoothly. The path length difference between the central and peripheral magnetic field lines (Fig. 3) is $0.156h$, where h is the length

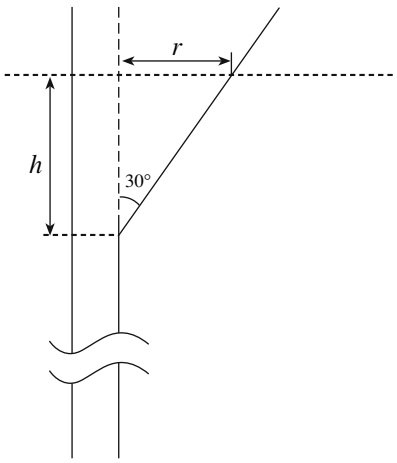

Fig. 3. Schematic view of the structure of umbral magnetic field lines illustrating the appearance of a Doppler signal phase delay in the "visual pattern" scenario.

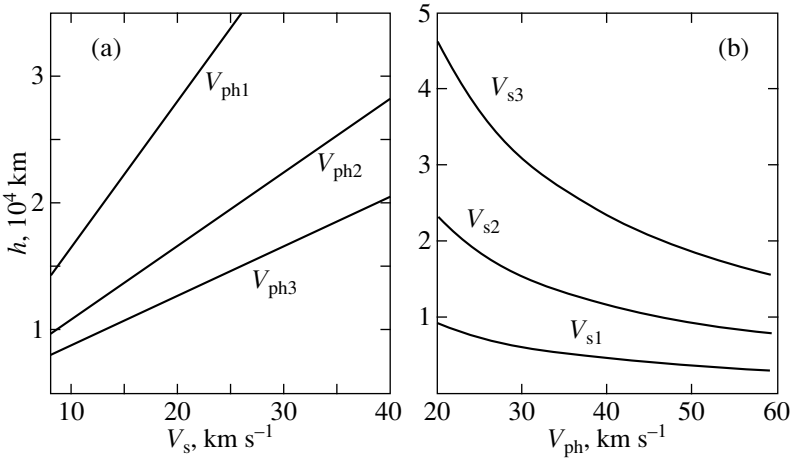

Fig. 4. To the determination of depth h: (a) h as a function of the speed of sound (calculated for three phase velocities, $V_{ph1} = 20$, $V_{ph2} = 40$, and $V_{ph3} = 60$ km s^{-1}); (b) h as a function of the measured phase velocity (calculated for three speeds of sound, $V_{s1} = 8$, $V_{s2} = 20$, and $V_{s3} = 40$).

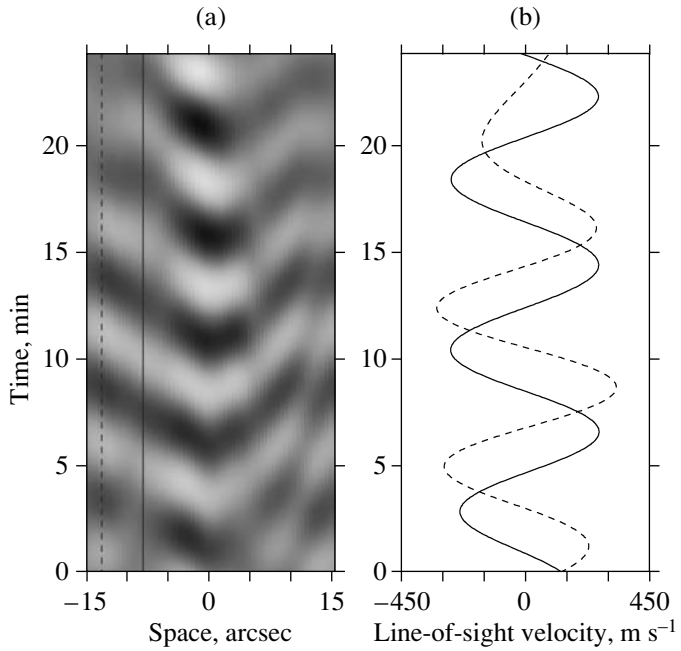

Fig. 5. Half-tone space–time line-of-sight velocity diagram for the five-minute mode of running penumbral waves: (a) chevron structures pointing to running penumbral waves; (b) phase delay of the signal measured at different penumbral points marked by the vertical lines in Fig. 5a.

of the central magnetic field line in the segment of phase delay accumulation. In other words, h is the minimum depth at which the peripheral magnetic field lines are already inclined at an angle of 30° to the vertical line. In a rough approximation, we can write $h/V_s = 6.4dT$, where V_s is the mean speed of sound from the beginning of the disturbance to the chromospheric layer observed in Hα. We can define the signal time delay as $dT = r/V_{ph}$, where r is the radius of the sunspot umbra (for medium-sized sunspots, r is about 4000 km) and V_{ph} is the measured phase velocity. In final form, we can write

$$h = 6.4\frac{V_s}{V_{ph}}r. \quad (1)$$

Using data from Lites and Skumanich (1982), Staude (1981), and Christensen-Dalsgaard et al. (1996), we will take speeds of sound of 8 km s^{-1} for the lower chromosphere, 20 km s^{-1} for the subsurface photosphere (200–300 km), and 40 km s^{-1} for the

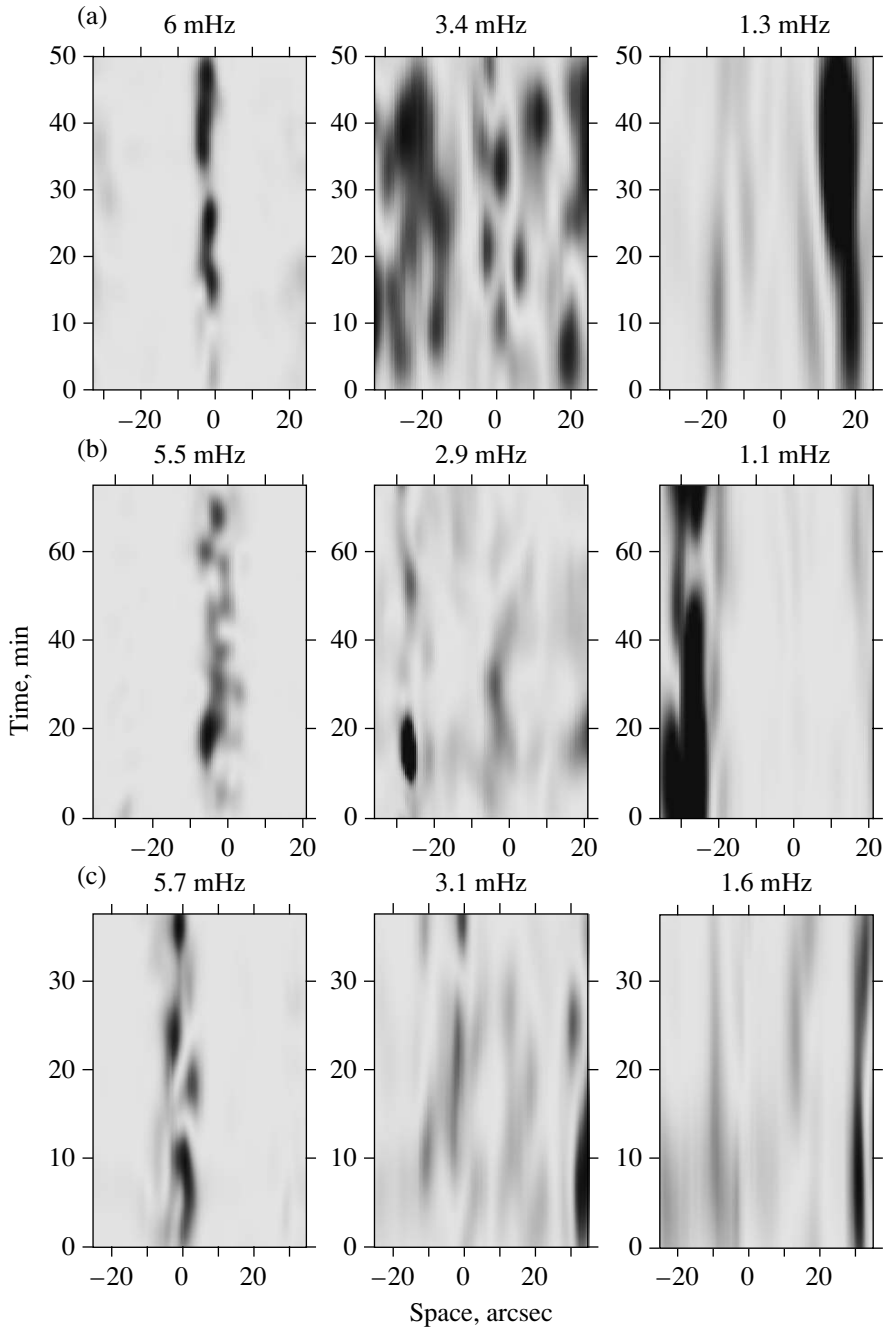

Fig. 6. Space–time Doppler velocity power diagrams for different frequency modes: (a) NOAA657, (b) NOAA791, and (c) NOAA794.

deeper layers. Substituting these values into (1) and specifying V_{ph} in the range of actually measured values (Tziotziou et al. 2006; Kobanov et al. 2006), we will obtain three curves reflecting the phase velocity dependence of the depth of the "acceleration" segment (Fig. 4b). In Fig. 4a, h is plotted against the speed of sound for three phase velocities (20, 40, 60 km s^{-1}).

We see from Fig. 4 that the low horizontal phase velocity in the sunspot umbra ($\sim$ 20 km s^{-1}) given by Tziotziou et al. (2006) requires a long path for the accumulation of the measured phase difference between the signals, which determines the very deep position of the oscillation source. It is hard to assume that the peripheral umbral magnetic field lines are already inclined at an angle of 30° at a depth of 10 000–30 000 km. These discrepancies arise from a difference in the measurements of the horizon-

tal phase velocity (signal time delay) in the umbral chromosphere. Our estimations of this velocity (40–70 km s^{-1}) lead to smaller depths. Note that our rough scheme yields only minimum estimates for the length of the "acceleration segment." Taking into account the curvilinearity of the peripheral filaments and the increase in the speed of sound with depth will lead to even higher values.

Note yet another interesting peculiarity encountered in the Hα observation of the umbral oscillations. The H$\alpha \pm 0.2$Å core is usually attributed to altitudes of 1500–2000 km, while the wings (H$\alpha \pm 0.6$ Å) are attributed to deeper layers, 600–900 km (Vernazza et al. 1981). One would think that the phase delay of the Doppler velocity signal recorded in the core relative to the signal in the wing is very easy to measure. At a speed of sound of 7–9 km s^{-1}, this delay should be about 100 s. In high-cadence observations, such a delay cannot go unnoticed. However, no direct and clear evidence for such a delay is provided in the present-day literature, despite the abundance of Hα observations.

Running Penumbral Waves

As was noted in the Introduction, the knottiest question is that of the connection between the three-minute umbral oscillations and the traveling penumbral waves. In our opinion, all of the difficulties with the transformation of the frequency of the waves and the velocity of their propagation in the penumbra are attributable to the simultaneous action of different frequency modes. When the frequency filtering of the main modes is applied, the picture becomes clearer. It becomes clearly seen in the halftone line-of-sight velocity diagrams that the traveling three-minute oscillations represented by the chevron structures (Fig. 1) are limited mainly by the umbra sizes, while the main mode of the running penumbral waves associated with the five-minute period (Fig. 5) is traceable up to the outer penumbral boundary. Previously, we provided arguments (Kobanov and Makarchik 2004; Kobanov et al. 2006) that the running penumbral waves are not an extension of the umbral waves. Here, we give new additional evidence for the absence of such a connection (Fig. 6). These figures show the space–time power distributions of the line-of-sight velocity oscillations constructed for individual frequency modes. The data used for these figures are based on high-cadence (0.5 s) observations of three different sunspots. The power maxima of these modes mostly have a different spatial localization. Whereas the three-minute mode is limited rather sharply by the spatial sizes of the umbra, the five-minute mode occupies the penumbra space. Longer-period oscillations are found near the outer penumbral boundary and even beyond it. In these figures, we will not find any temporal coordination in the appearance of maxima of individual modes that would indicate the frequency transformation as the wave propagates from the umbra into the outer penumbra either. Thus, it remains to recognize that the observed decrease in the RPW frequency results from the combined action of different frequency modes. The frequency autoselection of oscillations in the penumbra can be explained by a considerable difference in the inclination of the magnetic field lines as one recedes from the sunspot umbra (Bogdan and Judge 2006).

The five-minute oscillations with the measured amplitude of the line-of-sight velocity oscillations 150–250 m s^{-1}, which is an order of magnitude smaller than the amplitude of the umbral three-minute oscillations, is the main RPW mode. According to our measurements (Kobanov et al. 2006), the horizontal phase velocity determined from the line-of-sight velocity signal delay at different penumbral points lies within the range from 28 to 70 km s^{-1}. Note that 28 km s^{-1} is the minimum of all our measurements and was recorded only once. Such a large spread is clearly the result of a difference in the magnetic field topology of individual sunspots (torsion, etc.). However, within the penumbra of each sunspot, this parameter changes little. Note that our mean horizontal phase velocities in the penumbra also exceed the mean values given by Tziotziou (2006) by almost a factor of 3.

Let us attempt to determine what oscillations we observe in the Hα line in the penumbra. We will assume the penumbral magnetic field to be nearly horizontal. Suppose that we are dealing with acoustic oscillations that propagate along the horizontal magnetic field lines. Then, in the observations of one horizontal magnetic flux tube in the penumbra, we will record no line-of-sight velocity signal, because the oscillations take place across the line of sight. At the same time, the brightness oscillations, which are an essential attribute of acoustic oscillations, will be recorded. Note that the recorded horizontal phase velocity in the intensity signal should not exceed the speed of sound in the chromosphere (7–9 km s^{-1}) in this case. In contrast, we record a considerably higher propagation velocity, more clearly in the Doppler velocity signal, which should not be by definition.

Since Hα is an optically thick line and spans a certain range of altitudes, the line of sight in the penumbra can cross several horizontal magnetic flux tubes at different altitudes. In this case, the brightness fluctuations at different altitudes will lead to an asymmetry of the Hα profile, which will change synchronously with the oscillations. The latter can be recorded as a line-of-sight velocity signal and presents a problem for recognition. We will run into other difficulties if

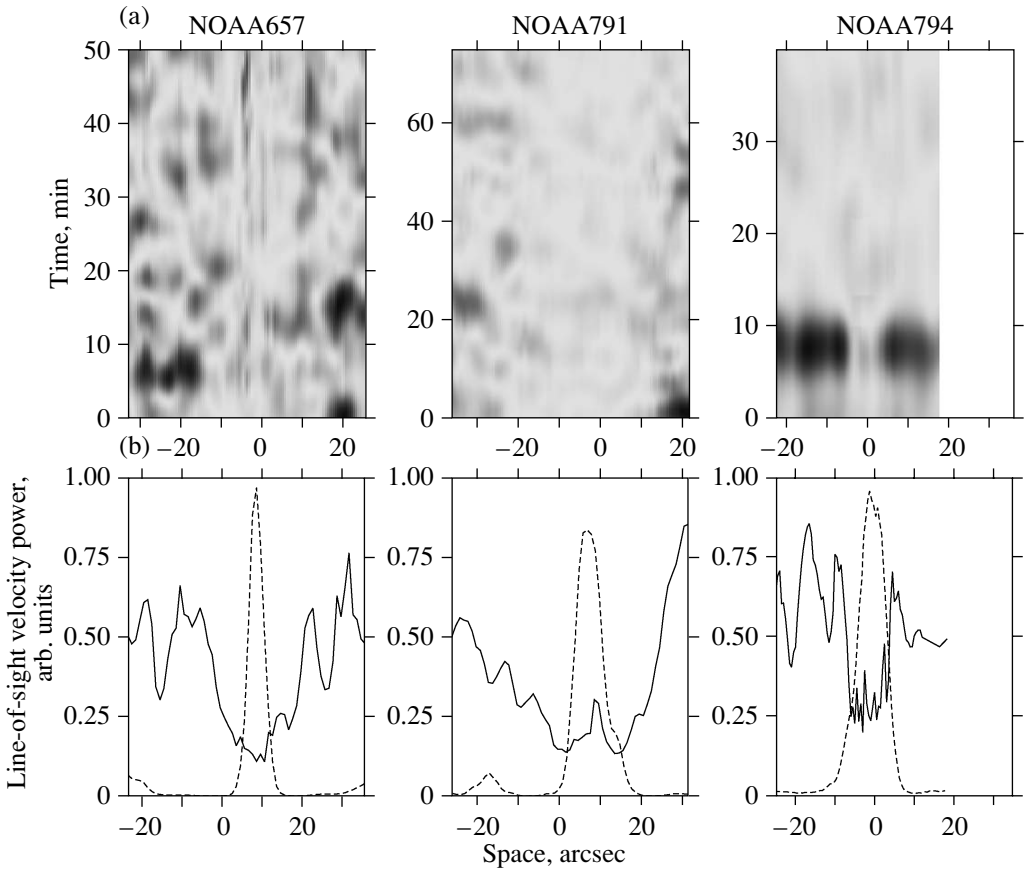

Fig. 7. To the illustration of the altitude inversion of the spatial localization of the three-minute oscillations: (a) space–time diagram of the three-minute oscillation power distribution in the photosphere of three sunspots; (b) time-averaged spatial three-minute oscillation power profiles (the solid and dotted lines are for the photosphere and the chromosphere, respectively).

we assume that the observed penumbral waves are Alfvén (kink-mode) ones; in this case, apart from the Doppler velocity oscillations, the oscillations in longitudinal magnetic field with sign reversal for the kink mode should also be recorded. However, there is no such information in the papers published to date.

According to present views, the sunspot penumbra consists of two types of filaments. Dark, almost horizontal filaments adjoin light, less inclined ones (Weiss 2006; Solanki and Montavon 1993; Thomas and Weiss 2004), which thread the Hα-controlled chromospheric layer. If the five-minute acoustic oscillations propagate along these inclined (but not horizontal) filaments, then the line-of-sight velocity signal can be recorded, though with an amplitude that is several times smaller because of projection effects. The path difference will appear between the oscillations propagating along the peripheral filaments and the filaments adjacent to the umbra. A visual pattern of radially traveling oscillations or what is called running penumbral waves will arise.

Altitude Inversion of the Spatial Localization of the Three-Minute Oscillations

The contradictions considered above by no means exhaust the entire problem related to the wave propagation in sunspots. Let us turn again to the waves observed in the umbral chromosphere. One would think that the "visual pattern" scenario considered above explains most satisfactorily the observed properties of the oscillations. According to this scenario, the three-minute oscillations are acoustic and are excited in deep subphotospheric layers by convective motions. One would then expect that the three-minute oscillations must be observed in the umbral photosphere, even if with a considerably smaller amplitude than in the chromosphere. In any case, their power should not be lower than that of the three-minute oscillations in the photosphere of the neighboring penumbra. Otherwise, it is unclear where the three-minute oscillations arise in the umbral chromosphere. Surprisingly, our observations show a completely different picture (Fig. 7). A dip in the sunspot umbra is detected in the space–time power diagrams of the three-minute photospheric oscillations. In the penumbral regions im-

mediately adjacent to the umbra, their power is much higher. The distributions presented in the figures were constructed by analyzing the time series pertaining to three different sunspots. One cannot but pay attention to the sharp decrease in the power of the three-minute photospheric oscillations precisely in the umbra. We called this effect an "altitude inversion of the spatial localization of the three-minute oscillations". We cannot yet give any acceptable explanation for this effect. An explanation should probably be sought in the new theory developed by Zhugzhda (2007).

CONCLUSIONS

Applying a separate analysis of the frequency modes to high-cadence observational data leads us to conclude that there is no transformation of the three-minute umbral waves into the five-minute penumbral ones. The horizontal propagation velocity of the disturbance in both umbra and penumbra is not related to the distance from the sunspot center and is 40–70 km s^{-1} in the umbra and 30–70 km s^{-1} in the penumbra.

The pattern of traveling waves in the umbral chromosphere is not constant and periodically passes into the pattern of standing waves.

For the 6-mHz frequency mode, we found an altitude inversion of the spatial power localization: the power minimum of the photospheric oscillations corresponds to the spatial coordinate of the oscillation maximum in the chromosphere.

ACKNOWLEDGMENTS

We wish to thank V.M. Grigor'ev for a helpful discussion and advice. This work was supported by the Russian Foundation for Basic Research (project no. 05-02-16325), the State Program for Support of Leading Scientific Schools of Russia (project no. NSh-4741.2006.2), and the Program of the Presidium of the Russian Academy of Sciences No. 16 (part 3, project 1.1).

REFERENCES

1. D. Banerjee, E. O'shea, M. Goossens, et al., Astron. Astrophys. **395**, 263 (2002).
2. J. M. Beckers and P. E. Tallant, Sol. Phys. **7**, 381 (1969).
3. T. J. Bogdan and P. G. Judge, Philos. Trans. R. Soc. London, Ser. A **364**, 313 (2006).
4. N. Brynildsen, P. Maltby, O. Kjeldseth-Moe, et al., Astron. Astrophys. **398**, L15 (2003).
5. N. Brynildsen, P. Maltby, C. R. Foley, et al., Sol. Phys. **221**, 237 (2004).
6. J. G. Doyle, E. Dzifcakova, and M. S. Madjarska, Sol. Phys. **218**, 79 (2003).
7. A. A. Georgakilas, E. B. Christopoulou, and H. Zirin, Bull. Am. Astron. Soc. **32**, 1489 (2000).
8. J. Christensen-Dalsgaard, W. Dappen, S. V. Ajukov, et al., Science **272**, 1286 (1996).
9. E. B. Christopoulou, A. A. Georgakilas, and S. Koutchmy, Astron. Astrophys. **354**, 305 (2000).
10. R. G. Giovanelli, Sol. Phys. **27**, 71 (1972).
11. N. I. Kobanov, Prib. Tekh. Éksp., No. 4, 110 (2001) [Instrum. Exp. Tech., No. 4, 592 (2001)].
12. N. I. Kobanov and D. V. Makarchik, Astron. Astrophys. **424**, 671 (2004).
13. N. I. Kobanov, D. Y. Kolobov, and D. V. Makarchik, Sol. Phys. **238**, 231 (2006).
14. B. W. Lites and A. Skumanich, Astrophys. J. **49**, 293 (1982).
15. E. O'Shea, K. Muglach, and B. Fleck, Astron. Astrophys. **387**, 642 (2002).
16. L. H. M. Rouppe van der Voort, Astron. Astrophys. **397**, 757 (2003).
17. S. K. Solanki and C. A. P. Montavon, Astron. Astrophys. **275**, 283 (1993).
18. J. Staude, Astron. Astrophys. **100**, 284 (1981).
19. J. H. Thomas and N. O. Weiss, Ann. Rev. Astron. Astrophys. **42**, 517 (2004).
20. K. Tziotziou, G. Tsiropoula, and P. Mein, Astron. Astrophys. **381**, 279 (2002).
21. K. Tziotziou, G. Tsiropoula, N. Mein, et al., Astron. Astrophys. **456**, 689 (2006).
22. K. Tziotziou, G. Tsiropoula, N. Mein, et al., Astron. Astrophys. **463**, 1153 (2007).
23. J. E. Vernazza, E. H. Avrett, and R. Loeser, Astrophys. J., Suppl. Ser. **45**, 635 (1981).
24. N. O. Weiss, Space Sci. **124**, 13 (2006).
25. Yu. D. Zhugzhda, Pis'ma Astron. Zh. **33**, 698 (2007) [Astron. Lett. **33**, 622 (2007)].
26. H. Zirin and A. Stein, Astrophys. J. **178**, 85 (1972).

Translated by G. Rudnitskii